



## **PRELIMINARY SOIL-SLIP SUSCEPTIBILITY MAPS, SOUTHWESTERN CALIFORNIA**

By D.M. Morton<sup>1</sup>, R.M. Alvarez<sup>1</sup>, and R.H. Campbell<sup>1</sup>

*Digital preparation by* K.R. Bovard<sup>1</sup>, D.T. Brown<sup>2</sup>, K.M. Corriea<sup>1</sup>, *and* J.N. Lesser<sup>3</sup>

*Prepared in cooperation with*  
CALIFORNIA GEOLOGICAL SURVEY

Open-File Report OF 03-17

2003

Any use of trade, product, or firm names is for descriptive purposes only and does not imply endorsement by the U.S. Government. This database, identified as "Preliminary Soil-Slip Susceptibility Maps, Southwestern California" has been approved for release and publication by the Director of the USGS.

U.S. DEPARTMENT OF INTERIOR  
U.S. GEOLOGICAL SURVEY

<sup>1</sup>U.S. Geological Survey  
Department of Earth Sciences  
University of California  
Riverside CA 92521

<sup>2</sup>Department of Earth Sciences  
University of California  
Riverside CA 92521

<sup>3</sup>U.S. Forest Service  
Department of Earth Sciences  
University of California  
Riverside CA 92521

# **Preliminary Soil-Slip Susceptibility Maps, Southwestern California**

D.M. Morton, R.M. Alvarez, and R.H. Campbell

U.S. Geological Survey  
Department of Earth Sciences  
University of California  
Riverside, California, 92521

## *Introduction*

This group of maps shows relative susceptibility of hill slopes to the initiation sites of rainfall-triggered soil slip-debris flows in southwestern California. As such, the maps offer a partial answer to one part of the three parts necessary to predict the soil-slip/debris-flow process. A complete prediction of the process would include assessments of “where”, “when”, and “how big”. These maps empirically show part of the “where” of prediction (i.e., relative susceptibility to sites of initiation of the soil slips) but do not attempt to show the extent of run out of the resultant debris flows. Some information pertinent to “when” the process might begin is developed. “When” is determined mostly by dynamic factors such as rainfall rate and duration, for which local variations are not amenable to long-term prediction. “When” information is not provided on the maps but is described later in this narrative. The prediction of “how big” is addressed indirectly by restricting the maps to a single type of landslide process – soil slip-debris flows.

The susceptibility maps were created through an iterative process from two kinds of information. First, locations of sites of past soil slips were obtained from inventory maps of past events. Aerial photographs, taken during six rainy seasons that produced abundant soil slips, were used as the basis for soil slip-debris flow inventory. Second, digital elevation models (DEM) of the areas that were inventoried were used to analyze the spatial characteristics of soil slip locations. These data were supplemented by observations made on the ground. Certain physical attributes of the locations of the soil slip- debris flows were found to be important and others were not. The most important attribute was the mapped bedrock formation at the site of initiation of the soil slip. However, because the soil slips occur in surficial materials overlying the bedrocks units, the bedrock formation can only serve as a surrogate for the susceptibility of the overlying surficial materials.

The maps of susceptibility were created from those physical attributes learned to be important from the inventories. The multiple inventories allow a model to be created from one set of inventory data and evaluated with others. The resultant maps of relative susceptibility represent the best estimate generated from available inventory and DEM data.

Slope and aspect values used in the susceptibility analysis were 10-meter DEM cells at a scale of 1:24,000. For most of the area 10-meter DEMs were available; for those

quadrangles that have only 30-meter DEMs, the 30-meter DEMs were resampled to 10-meters to maintain resolution of 10-meter cells. Geologic unit values used in the susceptibility analysis were five-meter cells. For convenience, the soil slip susceptibility values are assembled on 1:100,000-scale bases. Any area of the 1:100,000-scale maps can be transferred to 1:24,000-scale base without any loss of accuracy. Figure 32 is an example of part of a 1:100,000-scale susceptibility map transferred back to a 1:24,000-scale quadrangle.

### *Soil-Slip Susceptibility Maps*

These maps are a preliminary regional assessment of the relative susceptibility for initiating soil slip-debris flows during periods of intense winter rains in southwestern California (Figure 1). The area included in this assessment includes all or parts of the 1:100,000-scale Santa Barbara (Plate 1), Los Angeles (Plate 2), San Bernardino (Plate 3), Long Beach (Plate 4), Santa Ana (Plate 5), Oceanside (Plate 6), San Diego (Plate 7) and El Cajon (Plate 7) quadrangles. These maps are intended to serve as a preliminary guide to the spatial distribution of the static conditions that influence where debris flows can originate. The procedure is systematic and applicable over the entire region. However, the dynamic condition – spatial distribution, duration, and intensity of rainfall – will vary from storm to storm, and the map should be interpreted in a context of the duration and intensity variations within a specific storm.

Debris flows are a common and widespread phenomenon during periods of intense winter rainfall in southern California. The news media commonly uses ‘mudslides’ to refer to these and many other kinds of landslides. Most debris flows occur during winters with above normal rainfall, especially during ‘El Nino’ winters. They can cause considerable damage and result in loss of life. Debris flows can occur as isolated flows (Figure 2), in small numbers (Figure 3) or can number in the tens of thousands during a single ‘triggering’ rainfall (Figures 4 and 24). As an example of how numerous these debris flows can be, more than 40,000 debris flows were generated in a small part of Ventura and Los Angeles Counties in 1969.

These debris flows originate as small, shallow landslides (Figures 5, 6, and 7), commonly referred to as soil slips (e.g., Campbell, 1975, Kesseli, 1943). Most soil slips initiate as debris slide blocks with a form of an elliptical-shaped slab. Debris slide blocks are a form of translational slides in the Varnes (1978) landslide classification. Most soil slips disaggregate into debris flows, fluid slurries of soil and rock detritus that commonly converge in stream channels, where they flow down channel at various speeds for various distances. Unlike ‘bedrock’ or ‘deep-seated’ landslides that are generally recognizable for long periods of time, commonly thousands of years, soil slip-debris flow scars quickly ‘absorb’ into the ambient physiography (Figure 8) leaving little if any record of their prior existence. The most lasting record of the debris flows are deposits that accumulate on fans or as relatively steep ravine or gully fill.

Not included in this analysis are debris flows produced by other ‘triggering’ agents such as summer monsoon rainfall or water derived from melting snow. Also not included is any analysis of ‘bedrock’ or ‘deep-seated’ landslides that are the result of winter rains.

These ‘bedrock’ or ‘deep-seated’ landslides typically occur some time after the winter rains, commonly months later (Figure 9), although a few, relatively small ‘bedrock’ or ‘deep-seated’ landslides occur during or soon after the rains (Figures 10 and 11).

Soil slips pose relatively little hazard at the sites of initial failure, but the debris flows that form from them can be a serious hazard to people and structures in their flow paths. These maps depict only the point of origin of soil slips and do not address the subsequent course of a debris flow or the distance a debris flow will travel (Figure 12). Some of the flows are deposited on hillsides (Figure 13), others in stream channels (Figure 14), and yet others are deposited on low gradient alluvial fans at the mouth of drainages (Figures 15 and 16); these fans are generally steeper than common for water-laid deposits. Where a debris flow from a tributary enters a flowing stream, especially a stream already in flood, the sudden volume increase may produce a flood surge downstream (Figures 17 and 18). Subsequently, the particulates will become dispersed in the flood flow and eventually come to rest as alluvial deposits.

The soil-slip susceptibility map identifies those natural slopes most likely to be the sites of soil slips during periods of intense winter rainfall. The maps were largely derived by extrapolation of debris flow inventory data collected from selected areas of southwestern California. Excluded from this analysis are areas that have recently burned. Recently burned areas have exceptionally great potential for producing debris flows with little rainfall. Due to the change in physical properties of surface material during wildfires (e.g., DeBano, L.F., 1981, Morton, D.M., 1989, Rice, R.M., and others, 1972) any subsequent debris flow activity is markedly different from that of unburned areas. Surface material in recently burned areas is commonly hydrophobic and does not require saturation of the soil to form soil slips. In contrast to the debris flows produced by mobilization of soil slips, in recently burned areas the surface material is mobilized directly into debris flows and/or hyperconcentrated fluvial stream channel flows. Much of the material constituting these debris flows is derived from debris at the base of slopes and/or debris already in the channel. In recently burned areas debris-flow activity has been associated with as little as 0.25 in. rainfall. Two areas known to us that burned during the summer and fall of 2002 are outlined on the 1:100,000-scale San Bernardino quadrangle. Any other recently burned areas should be considered as having great potential for producing debris flows and/or hyperconcentrated fluvial flows.

The soil-slip susceptibility analysis applies only to natural slopes. The base topographic maps (U. S. Geological Survey 7.5’ quadrangles) used in this analysis do not accurately identify man-modified slopes. Although the 7.5’ quadrangles indicate urbanized areas (termed, ‘built-up areas’ on the 7.5’ topographic maps), for most if not all of the 7.5’ quadrangles there has been additional hillside development since the publication of the quadrangle. Susceptibility values are only for natural slopes and *do not* apply to any man-modified slopes.

### *Debris Flow Model*

The basic model used for the origin of soil slips is Kesseli’s (1943), amplified and applied to winter rain generated soil-slips in southern California by Campbell (1975);

figure 19). In this model, when infiltration of water into the soil exceeds the transmissive capacity of the bedrock, a perched water table above the bedrock can develop, saturating a zone above the colluvium-bedrock interface to create an interconnected hydraulic system. As the thickness of this saturated zone increases, the pore pressure at the potential slip surface increases, and the soil layer can fail by rupture along or above the soil-bedrock interface producing a soil slip (Campbell, 1975). The saturated material of most soil slips liquifies on down-slope displacement forming a debris-flow slurry that continues down slope. The transformation can be considered a form of liquefaction under monotonic strain (Poulos and others, 1985, see fig. 10). Some debris flows disintegrate over the slope below, leaving scattered clumps and clods of soil (figures 13 and 20). But many enter first order stream channels and continue to flow down channel, where they can add saturated channel-fill material to their volume.

A detailed analysis was made of 11,560 debris flows that occurred during the winters of 1927, 1969, and 1998 in the Santa Paula area, Ventura County. The average length of debris flows was 180-200 feet; the shortest debris flows were about 3 feet in length and the longest were about 2,200 feet. Although most flows travel only 200 – 400 feet down slope, many progress through first order channels into higher order stream channels, where merged debris flows can travel a considerable distance. In 1969 some debris flows in Ventura County traveled 6,000 to 8,000 feet down channels. Where higher order channels are carrying significant stream-flow, debris flows may be diluted so that deposits cannot be distinguished from alluvial deposits.

### *Rainfall*

For the events studied by Campbell (1975) about 10 inches of antecedent rainfall was needed before soil-slips were generated, implying regional achievement of field capacity. Subsequent rainfall with intensity of 0.2-0.25 in./hr for an hour or more was required to develop soil slips. This indicates that, even if of light intensity, rainfall can wet the colluvium (hillside surface layer composed of soil and rock fragments) to the point that additional heavy rain will cause a zone above the colluvium-bedrock interface to saturate, forming a perched water table. For the San Francisco Bay area Cannon and Ellen (1988) found variation in mean annual precipitation governed the amount and intensity of rainfall needed to produce soil slips. For areas with a mean annual precipitation of less than 26in. abundant debris flows were generated after 15 –19in. of pre-storm rainfall and 17 hrs of intense rainfall of 0.1-0.25in. /hr. For areas with a mean annual precipitation greater than 26in. abundant debris flows were generated after 20-30in. of pre-storm rainfall and 8 hrs of intense rainfall of 0.4-0.8in. /hr. Most of coastal southern California receives less than 26in. mean annual precipitation. However, southern California has a pronounced orographic variation in mean annual precipitation, which ranges from about 10 in. to as much as 40 in. in higher elevation mountain areas. (Mean annual precipitation maps for southern California are given at a State of California website, <http://frap.cdf.ca.gov/data/frapgisdata/select.asp> and in Minnich and Everett (2002). In southern California there appears to be a relationship between mean annual precipitation and rainfall necessary to generate soil slips. In general, for every one inch increase in mean annual precipitation an additional two inches of rainfall above ten inches is required to generate soil slips.

## *Debris Flow Inventories*

Used in the development of these soil slip susceptibility maps were soil slip-debris flow inventory maps that were made in a variety of geologic, geomorphic, and climatic settings in southwestern California. The primary data set were maps of debris flows that were generated during 1998. Mapping was on aerial photography transects that sampled a variety of geologic, geomorphic, and ecological settings between Santa Barbara and northern San Diego County. Debris flows in most of the transects were only generated during a single storm. However, for some transects in parts of Los Angeles and Ventura Counties, there were several storms that generated debris flows. For these transects aerial photography was repeated after each storm that generated debris flows. Some inventory photography was obtained for part of Ventura and Santa Barbara Counties in 2001. Supplementing the 1998 and 2001 debris flow inventory maps are 1969 debris flow inventory maps for part of Ventura and Los Angeles Counties (Morton, 1976a, 1976b, 1976c), unpublished debris flow maps in Ventura County for 1927, 1939, 1941, and 2001, in the Sunland area, Los Angeles County for 1969, and 1979, in the San Timoteo Badlands area, Riverside County for 1939, and in southern Orange County in 1969. Debris flow inventory maps were made by identification of debris flows on aerial photographs with a nominal scale of 1:24,000. Debris flow lines were transferred by inspection to 7.5' U.S. Geological Survey quadrangle maps and digitized into a geographic information system (GIS) using Arc/Info. Debris flows are represented as one-dimensional line features. Each digitized debris flow line follows the flow direction from the up-slope point of origin down to the flow terminus. The location of the soil slip scar is taken as the up-slope point of origin for the debris flow.

## *Analysis*

Detailed spatial analyses of the digitized soil slips were made in the Santa Paula area, Ventura County, for the winters of 1927, 1969, 1998, and 2001, the Sunland area, Los Angeles County, for the winters of 1969, 1979, and 1998, and the San Timoteo Badlands area, Riverside County, for the winters of 1939, 1969, and 1998. Black-and-white archive aerial photography was used for 1927, 1969, and 1979 inventories. Color aerial photography was obtained for the areas outlined in Figure 1 after soil slip-debris flow generating rainfall in 1998 and 2001.

Based on the spatial analyses of soil slips, three factors in addition to rainfall were found to be most important in the origin of soil-slips. These factors are geology, slope, and aspect. Vegetation and slope concavity-convexity were less important factors and were not included in the development of the soil slip susceptibility map. In other areas both slope concavity-convexity (e.g., Ellen, 1988) and vegetation (e.g., Wiczorek and Sarmiento, 1988) apparently exert important controls. In this analysis vegetation is *de facto* included because in much of the lower elevation areas of southwestern California, especially semi-arid areas, vegetation type is largely controlled by aspect – relatively shallow rooted grass-dominated south-facing slopes and more deeply rooted chaparral – and/or tree-dominated north-facing slopes.

## *Geologic Units*

Analyses of soil-slip inventories in southern California indicate a direct relationship between soil developed on geologic map units and the occurrence of soil slip-debris flows (Figures 21, 22, 23, and 24). Use of “geologic map unit” refers to the soil or colluvium developed on the mapped unit, not the subsoil lithology.

The geologic map data sources used were the San Diego, Long Beach, and Oceanside 1:100,000-scale quadrangles (in preparation) of the California Geological Survey, and the Santa Ana (Morton, 1999) and Los Angeles and San Bernardino 1:100,000-scale quadrangles (in preparation) of the U.S. Geological Survey. Most of the line work in these 1:100,000-scale quadrangles is accurate at 1:24,000-scale. Weber’s 1:62,500-scale map (1973) was used for southern Ventura County. In the Santa Barbara area the 1:24,000-scale map of Minor and others (2000) was used. Geologic map data were sampled on a five-meter grid; the small size of the grid was selected to best preserve the integrity of the digital geologic data.

## *Slope and Aspect*

Slope has long been recognized as a critical factor in generating soil slips (e.g., Campbell, 1975, Campbell, and others, 1989, Morton, 1976d). In southern California a clear relationship exists between frequency of soil slips and slope. As an example in the Santa Paula area, Ventura County, 70% of 5,177 debris flows originated in 10 meter DEM cells with slopes between 20° and 36° (Figure 25). The 70% is a low percentage due to artifacts in slope calculations; an additional 20% of the debris flows originated on equally steep slopes near ridge tops, but whose calculated slope values were lower as the slope calculation includes low-slope ridge-top cells.

In previous studies aspect has generally not been included in analysis of soil-slip susceptibility. However, debris flow analyses in the Santa Paula area, Ventura County (Hauser, 2000), Sunland area, Los Angeles County (Koukladas, 1999), and the San Timoteo Badlands area, Riverside County (unpublished data) indicate more debris flows occur on south-facing slopes than on north-facing slopes (Figures 26, 27, and 28). Commonly south-facing slopes in southern California support less biomass than north-facing slopes. Poole and Miller (1975) found for an inland area near Descanso, San Diego County, soil moisture content was higher on south facing slopes than on north-facing slopes, but slope differences were not as clear in a coastal area at Camp Pendleton, San Diego County. Apparently, greater evapotranspiration removes more soil moisture on the north-facing slopes with greater biomass than on south-facing slopes with less biomass. The tendency for north-facing slopes to fail less frequently than those facing south may be due to lower moisture in the soil coupled with generally greater density and depth of roots on the north-facing slopes.

Slope and aspect data were derived from U.S. Geological Survey 1:24,000-scale 10-meter and 30-meter DEMs (Figure 29) resampled to 10-meters, using Arc/Info grids and Grid functions (Environmental Systems Research Institute, 1998). Ten meter DEMs were available for the Los Angeles, Long Beach, and Santa Ana 1:100,000-scale quadrangles.

Only 30-meter DEMs were available for the western four 7.5' quadrangles in the Santa Barbara 1:100,000-scale quadrangle, the Dos Pueblos Canyon, Goleta, Santa Barbara, and Carpinteria quadrangles. For the San Bernardino quadrangle a 30-meter DEM was used for the Keller Peak 7.5' quadrangle; 10-meter DEMs were used for the remaining 15 7.5' quadrangles. For the Oceanside 1:100,000-scale quadrangle six 10-meter DEMs were available (Dana Point, San Clemente, Fallbrook, Temecula, Rancho Santa Fe, and Escondido 7.5' quadrangles), and only 30-meter DEMs were available for the remaining 11 quadrangles (Margarita Peak, San Onofre Bluff, Las Pulgas Canyon, Morro Hill, Bonsall, Pala, Oceanside, San Luis Rey, San Marcos, Valley Center, and Encinitas 7.5' quadrangles). Only 30-meter DEMs were available for the San Diego and El Cajon 1:100,000-scale quadrangles. Use of resampled 30-meter DEMs can produce an artificial rectilinear pattern of soil slip susceptibility values in areas with little relief, such as the coastal part of the Oceanside and San Diego 1:100,000-scale quadrangles.

### *Susceptibility Values*

Soil-slip susceptibility values are a product of the numerical values assigned to the geologic map units, slope, and aspect. Numerical values ranging from zero to 25 were assigned to geologic map units. Assigning geologic unit values is based on analysis of debris flow inventory maps augmented by field observations by the authors for the period 1969 through 2001. The field observations of debris flow distribution were made for a large variety of geologic map units under varying rainfall conditions.

Some geologic map units have not been observed to produce soil-slips or produce deposits recognizable as the product of debris flows. These map units are given a zero susceptibility value. Most of the zero value geologic units are very young alluvial deposit units, and in the Oceanside and Santa Ana 1:100,00-scale quadrangles, granitic rock units. The most susceptible units are given a value of 25, the least susceptible units, except for the zero susceptibility units, are assigned a value of 5. Intermediate susceptibility values are assigned on the basis of observed relative susceptibility. Although there is a great deal of subjectivity in assigning values to individual geologic units, the inventory maps indicate a relative difference in the rainfall required to initiate soil slips in different geologic units. The assigned values are based upon the inventory maps and ground inspection during 1969, 1998, and 2001 winter rains. For geologic units not included within the mapped areas soil slip susceptibility values were assigned on the basis of lithologic similarities. Zero values were assigned to geologic map units in which debris flows have not been observed.

Slope is considered to be equal in importance with geology and given the same range of values as geologic values, zero to 25. The zero value is based upon the inventory maps where no soil slips were found to originate on DEM derived slopes under  $2^{\circ}$ . Slope interval values and percentage of soil slips per slope interval for 1998 in the Santa Paula area is  $2^{\circ}$ - $13^{\circ}$ , 1.5%;  $13^{\circ}$ - $19^{\circ}$ , 10%;  $20^{\circ}$ - $36^{\circ}$ , 82%;  $37^{\circ}$ - $42^{\circ}$ , 5%;  $>43^{\circ}$ , 1.5%. Numerical values were assigned to the slope intervals based on the percentage of soil slips in the intervals;  $<13^{\circ} = 0.6$ ;  $13^{\circ}$ - $19^{\circ} = 3$ ;  $20^{\circ}$ - $36^{\circ} = 25$ ;  $37^{\circ}$ - $42^{\circ} = 2$ ;  $>43^{\circ} = 0.6$ .

Analyses of the inventory data also show that some orientations of aspect are associated with greater frequency of debris flows than are other orientations. But, aspect is a less important factor in determining the sites of soil slips than slope and geology. The relative importance of aspect with respect to geology and slope is reflected in the assigned range of aspect values. Based on spatial analyses, assigned aspect values range from 2-8. The relative importance of different orientations is reflected in the assigned values for different aspect intervals. From 360<sup>0</sup>, north, aspect intervals and assigned values are 0<sup>0</sup>-74<sup>0</sup>, 2; 75<sup>0</sup>-145<sup>0</sup>, 6; 145<sup>0</sup>-220<sup>0</sup>, 8, 220<sup>0</sup>-290<sup>0</sup>, 6; and 290<sup>0</sup>-360<sup>0</sup>, 2.

The derived soil slip susceptibility values are the product of the geology, slope, and aspect. The larger the susceptibility value, numerically, the greater the potential to produce soil-slips. The consequent range in soil-slip susceptibility values is zero to 5,000 ( $25[\text{geology}] \times 25[\text{slope}] \times 8[\text{aspect}] = 5,000$ ). For cells not having a zero value for geology and/or slope, the smallest value is 6 ( $5[\text{geology}] \times 0.6[\text{slope}] \times 2[\text{aspect}] = 6$ ). Soil slip susceptibility values were calculated for 128 7.5' quadrangles; 100 7.5' quadrangles with 10-meter DEMs and 28 7.5' quadrangles with resampled 30-meter DEMs. The resampled 30-meter DEMs give rise to less accurate analysis, and artifacts may be more easily included; this is most apparent in the gently sloping coastal part of the Oceanside and San Diego quadrangles. The 7.5' quadrangle soil-slip susceptibility values were assembled on 30'x60' quadrangle bases. Four susceptibility value units plotted are: zero susceptibility; low susceptibility values, 6-999; moderate susceptibility values, 1,000-3,250; high susceptibility values, 3,251--5,000. For the Santa Paula area, based on a least squares fit of the percentage of cells with soil slips to susceptibility values, 0.15 to 0.85 % of the low susceptibility value cells had soil slips, 0.85 to 2.5% of the moderate value cells had soil slips, and 2.5 to 3.7% of the high value cells had soil slips (Figure 30).

Detailed spatial analyses of the distribution of soil slips were made in the Santa Paula area, Ventura County, Sunland area, Los Angeles County, and San Timoteo Badlands area, Riverside County. The analyses were conducted by comparing the actual distribution of soil slips determined from inventories with the distribution of low and medium susceptibility areas predicted from the model. It is expected a small percentage of the soil slips would occur in the low susceptibility class and these soil slips should be scattered about. Surprisingly, however, the soil slips in the low susceptibility class markedly cluster in areas adjacent to high susceptibility areas (e.g., Figures 31 and 32).

This clustering of soil slips in the low susceptibility class adjacent to high susceptibility areas apparently comes from the way slope inclination is calculated from a DEM. Most of the clustered soil slips in question actually occur in cells near the crests of steep slopes adjacent to the crest of the slope. Calculation of slope inclination integrates elevation data from the eight cells surrounding the cell for which the slope is being calculated. This integration effectively reduces the numerical value of slopes in cells where breaks in slope occur and is lower than would be measured in the field at the site of a soil slip. The nearest 10-meter cells to the break-in-slope at the head of a canyon or a ridge top has a calculated slope angle that is less than exists for that cell. This problem can be addressed by adding a 10-meter buffer to the areas of moderate and high susceptibility. For 1998 in the Santa Paula area, 69% of the soil slips occurred in the two highest susceptibility value

cells. An additional 25% of the soil slips for a total of 94% occurred within a 10-meter cell expansion of the moderate and high susceptibility valued cells. For 1998 in the Sunland area, 55 % of the soil slips occurred in the two highest susceptibility value cells. An additional 26% of the soil slips, for a total of 81%, occurred within a 10-meter cell expansion of the moderate susceptibility valued cells. For 1998 in the San Timoteo Badlands area, 53% of the soil slips occurred in the two highest susceptibility value cells. An additional 34 % of the soil slips, for a total of 86.5%, are included within an additional 10-meter expansion beyond the moderate susceptibility valued cells. Most of the soil slips included within the additional 10-meter cell expansion occurred near the crest of ridges reflecting the high percentage of soil slips that developed high on slopes. (FOOTNOTE: It is worthwhile to note that the abundance of soil soil-slip sites so near the crest of a slope (e.g., Figure 27) is evidence that subsurface down-slope flow of water is not particularly important here. If subsurface interflow were important, the sites of initiation would be expected farther downhill. Likewise, soil slips would be expected to concentrate more on concave rather than convex slopes where interflow concentrates subsurface water and elevates pore pressure. The analyses of factors significant to soil-slip initiation did not find slope shape to be very significant.)

### *Uncertainty factors*

A number of factors preclude development at this time of a more accurate soil slip-debris flow susceptibility map.

Geologic contacts on the geologic maps used are not always accurately located due to a variety of reasons including variations in interpretations of different geologists. There commonly is a difference in geologic map unit designation from geologist to geologist and the geologic maps used were compiled from the work of many geologists. Physical properties within geologic units differ from place to place within the map unit. This variation is due to a number of inherent factors including stratigraphic variation, facies changes, degree of induration, jointing or fracturing, and weathering. In this analysis very young alluvial units are considered to not develop soil slips. However, some geologic maps apparently lump younger and older alluvial deposits under a younger alluvial deposit designation; this can lead to a zero geologic value resulting in a zero susceptibility value rather than a higher value (e.g., Figure 31).

Some time is required for an existing soil slip scar to recover before another soil-slip can occur at that site. Due to lack of data this variable is not included in the derivation of the soil slip susceptibility analysis. The length of recovery time is a function of the parent material and climatic or microclimatic setting. Sites of 1998 soil slips are not expected to produce soil slips in 2003; however unfailed 1998 sites may yield soil slips in the same drainage; therefore the potential hazard in the drainage is not lessened. In the Santa Paula area, Ventura County, some sites of soil slips of 1927 appeared to be sites of soil slips in 1969 suggesting some parent material recovery time may be on the order of 40 years (Hauser, 2000).

Accuracy in the plotting and digitization of debris flows is a function of the quality of the base map and the skill of the individual doing the plotting and digitizing. Plotting the starting point of debris flows can be off by +/- one or two 10-meter DEM cells.

A DEM consists of regularly spaced elevation data at 10-meter (or 30-meter) intervals. The quality of the DEM is a function of the source data and process used in their construction. The quality as well as the resolution of the 30-meter DEMs is considerably less and more variable than that of the 10-meter DEMs. Detailed information on the vertical and horizontal accuracy, source data, and the process of creating DEMs is given in the U.S. Geological Survey's Data Users Guide 5, Digital Elevation Models, 1987. Slope angles calculated from DEMs are likely to vary from slope angles measured in the field. This difference is due to the smoothing effect of representing continuous data as regularly spaced points and any errors that exist in the source data that are used to generate the DEMs. As indicated above, calculation of slope for a cell at the head of a canyon or the uppermost side of a ridge gives rise to a specious low slope value.

### *Suggested uses and caveats*

This map covers a large region, within which the areas of greatest potential for hazard are identified. It does not directly identify all sites that have a potential for hazard from debris flows; only sites where debris flows may be expected to begin. However, it seems clear that sites in the flow paths below drainage basins containing large numbers of susceptible cells are more likely to be affected than those below drainages in which low to moderately susceptible cells predominate. Therefore, the map may help identify locations where the relative potential for hazard is greater, especially if evaluated in a context of weather forecasts reporting storm track location and direction, and expected rainfall rates and durations.

Emergency preparedness might be improved by the identification of areas where evacuation might be recommended if heavy rainfall conditions are expected. Areas that might become isolated by debris flows during a storm may need stocks of emergency food and medical supplies. Emergency shelters should not be located in flow paths below watershed areas having high susceptibilities. Locations where transmission and transportation corridors lie across flow paths from susceptible drainage basins might indicate sites where defensive works should be constructed.

Emergency response workers may be able to use the map as a guide to forecasting locations that may need more or less in the way of emergency resources. During a heavy rainstorm it may help avoid situations where rescue workers could be trapped, isolated, or otherwise impacted. In conjunction with a map of forecast storm rainfall distribution, the map may be of help in selecting areas where the worst damage or most serious isolation is to be expected.

Recovery and reconstruction could be aided by knowing the areas most likely to be impacted. Priorities for building permits, and the implementation of grading code restrictions, may be influenced.

## *Acknowledgements*

We appreciate useful input and critical comments from Kelly Bovard, U.S. Geological Survey, Jim Davis, Mike Kennedy, and Chris Wills, California Geological Survey, and Bob Graham, University of California, Riverside. Special thanks to Bob Fleming and John Sutter, U.S. Geological Survey, for substantial thoughts and input on the project and the map explanation. This work was conducted under the auspices of the National Cooperative Geologic Mapping Program, U.S. Geological Survey.

## *References*

Arc/Info, Version 7.1.1, 1998, Environmental Systems Research Institute, Inc., 380 New York Street, Redlands, California

Campbell, R.H., 1975, Soil slips, debris flows, and rainstorms in the Santa Monica Mountains and vicinity, southern California: Professional Paper 851, 51 p.

Campbell, R.H., Varnes, D.J., Fleming, R.W., Hampton, M.A., Prior, D.B., Sangrey, D.A., Nichols, D.R., and Brabb, E.E., 1989, Landslide classification of mud flows and other landslides: *in* Sadler, P.M., and Morton, D.M., eds., Landslides in a semi-arid environment with emphasis on the Inland Valleys of southern California, p. 1-27.

Cannon, S.H., and Ellen, S.D, 1988, Rainfall that resulted in abundant debris-flow activity during the storm, *in*, Landslides, floods, and marine effects of the storm of January 3-5, 1982, in the San Francisco Bay region, California, Ellen, S.D, and Wieczorek, eds.: U.S. Geological Survey Professional Paper 1434, p. 27-33.

DeBano, L.F., 1981, Water repellent soils: A state-of-the-art: Pacific Southwest Forest and Range Experiment Station, General Technical Report PSW-46, 21 p.

Digital elevation models, Data users guide 5, 1987: U.S. Geological Survey, Reston, Virginia.

Ellen, D.E., 1988, Distribution of debris flows in Marin County, *in*, Landslides, floods, and marine effects of the storm of January 3-5, 1982, in the San Francisco Bay region, California, Ellen, S.D, and Wieczorek, G.F., eds.: U.S. Geological Survey Professional Paper 1434, p. 113-132.

Hauser, R.M., 2000, Soil slip-debris flows during the winters of 1926-27, 1968-69, and 1997-98 in the Santa Paula area, Ventura County, California: Riverside, California, University of California, M.S. thesis, 64 p.

Kesseli, J.E., 1943, Disintegrating soil slips of the Coast Ranges of Central California: *Journal of Geology*, v. 51, no. 5, p. 342-352.

Koukladas, Catherine, 1999, Lithologic and slope aspect controls on infinite slope failures in the western San Gabriel Mountains, Los Angeles County, southern California: Reno, Nevada, University of Nevada, M.S. thesis, 199 p.

Minnich, R.A., and Everett, R.G., 2001, Conifer tree distribution in southern California: *Madrono*, v. 48, no. 3, p. 177-197.

Minor, S.A., Kellogg, K.S., Stanley, R.G., Stone, P., Powell, II, C.L., Gurrola, L.D., Selting, A.J., and Brandt, T.R., 2002, Preliminary geologic map of the Santa Barbara coastal plain area, Santa Barbara County, California: U.S. Geological Survey Open-file Report 02-136.

Morton, D.M., 1976a, Reconnaissance surficial geologic maps of the Newhall, Oat Mountain, Santa Susana, and Val Verde 7.5' quadrangles, Los Angeles and Ventura Counties, California: U.S. Geological Survey Open-file Map 76-210.

Morton, D.M., 1976b, Reconnaissance surficial geologic maps of the Fillmore, Moorpark, Piru, and Simi 7.5' quadrangles, Ventura County, California: U.S. Geological Survey Open-file Map 76-212.

Morton, D.M., 1976c, Reconnaissance surficial geologic maps of the Santa Paula, Santa Paula Peak, Saticoy, and Ojai 7.5' quadrangles, Ventura County, California: U.S. Geological Survey Open-file Map 76-212.

Morton, D.M., 1976d, Relation between the distribution of 1969 storm-generated soil slips, pre-1969 landslides, and slope angle in part of southern California: *Geological Society of America Abstracts with Programs*, v. 8, no. 3, p. 398.

Morton, D.M., 1989, Distribution and frequency of storm generated soil slips on burned and unburned slopes, San Timoteo Badlands, southern California: *in* Sadler, P.M., and Morton, D.M., eds., *Landslides in a semi-arid environment with emphasis on the Inland Valleys of southern California*, p. 279-284.

Morton, D.M., 1999, Preliminary digital geologic map of the Santa Ana 30' x 60' quadrangle, southern California, version 1.0: U.S. Geological Survey Open-file Report 99-172.

Poole, D.K., and Miller, P.C., 1975, Water relations of selected species of chaparral and coastal sage communities: *Ecology*, v. 56, p. 1118-1128.

Poulos, S.J., Castro, Gonzalo, and France, J.W., 1985, Liquefaction evaluation procedure: *Journal of Geotechnical Engineering*, v. 111, no. 6, p. 772-791.

Rice, R.M., Rothacer, J.S., and Megahan, W.F., 1972, Erosional consequences of timber harvesting: An appraisal: *Proceedings National Symposium on watersheds in transition*, Fort Collins, Colorado, June 1972, American Water Resources Association, p. 321-329.

Varnes, D.J., 1978, Slope movement types and processes, in Schuster, R.L., and Krizek, R.J., eds., *Landslides – analysis and control*: National Academy of Sciences Transportation Research Board Special Report 176, p. 12-33.

Weber, F.H., Jr., 1973, Geology and mineral resources study of southern Ventura County, California: California Division of Mines and Geology Preliminary Report 14, 102 p.

Wieczorek, G.F., and Sarmiento, John, 1988, Rainfall, piezometric levels, and debris flows near La Honda, California, in storms between 1975 and 1983, *in*, Landslides, floods, and marine effects of the storm of January 3-5, 1982, in the San Francisco Bay region, California, Ellen, S.D, and Wieczorek, eds.: U.S. Geological Survey Professional Paper 1434, p. 43-62.

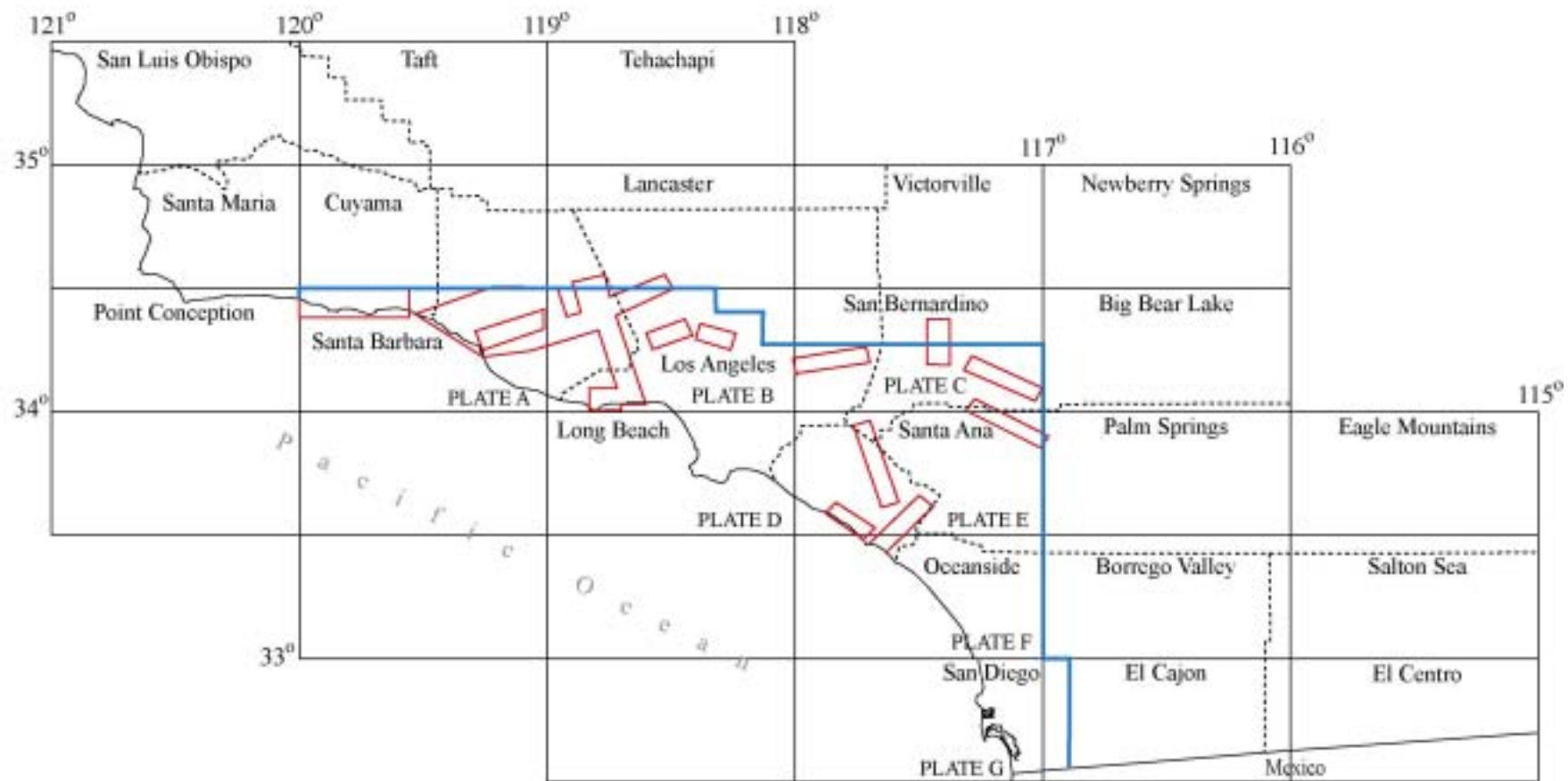


Figure 1 Index map of the Southern California Areal Mapping Project area (SCAMP). Outlined in blue is the area of soil-slip susceptibility 1:100,000-scale maps. The dashed lines are county boundaries and the red boxes outline areas covered by 1998 aerial photography.



Figure 2 Debris flow, Monterey Park, Los Angeles County, 1980. Debris flow is in Pleistocene alluvial deposits.



Figure 3 Multiple debris flows, Repetto Hills area, Los Angeles County, 1980. Debris flows are in Pleistocene alluvial deposits. Plastic sheets cover the upper parts of the debris flows.



Figure 4 Debris flows, Ventura, 1983. Debris flows are in the San Pedro and Santa Barbara Formations.



Figure 5 Soil slip, Las Cruces area, Santa Barbara County, 1998. Soil slip has remained intact.



Figure 6 Soil slip, Las Cruces area, Santa Barbara County, 1998. Lower right side of soil began to desintegrate. Located in upper left corner is soil slip scar.



Figure 7 Multiple soil slips, Wheeler Canyon, Ventura County, 1998. Note that the soil slips originated near the crest of the ridge. Soil slips in the lower photograph started to mobilize into debris flows.



Figure 8 Debris flow, Las Cruces area, Santa Barbara County, March 2001. The left hand photograph (a) taken the day the debris flow occurred. The right hand photograph (b) taken one year later, March 2002 (cows for scale).



Figure 9 'Bedrock' landslide, San Timoteo Badlands, Riverside County, 1999. Landslide occurred almost one year after the 1998 'El Nino' rains.



Figure 10 'Bedrock' landslide, Santa Monica Mountains, 1980. Landslide apparently due to undercutting of stream bank during winter rains.



Figure 11 Shallow incipient 'bedrock' landslides, Lake Cachuma area, Santa Barbara County, 1998. Landslide occurred during the 1998 'El Nino' rains.

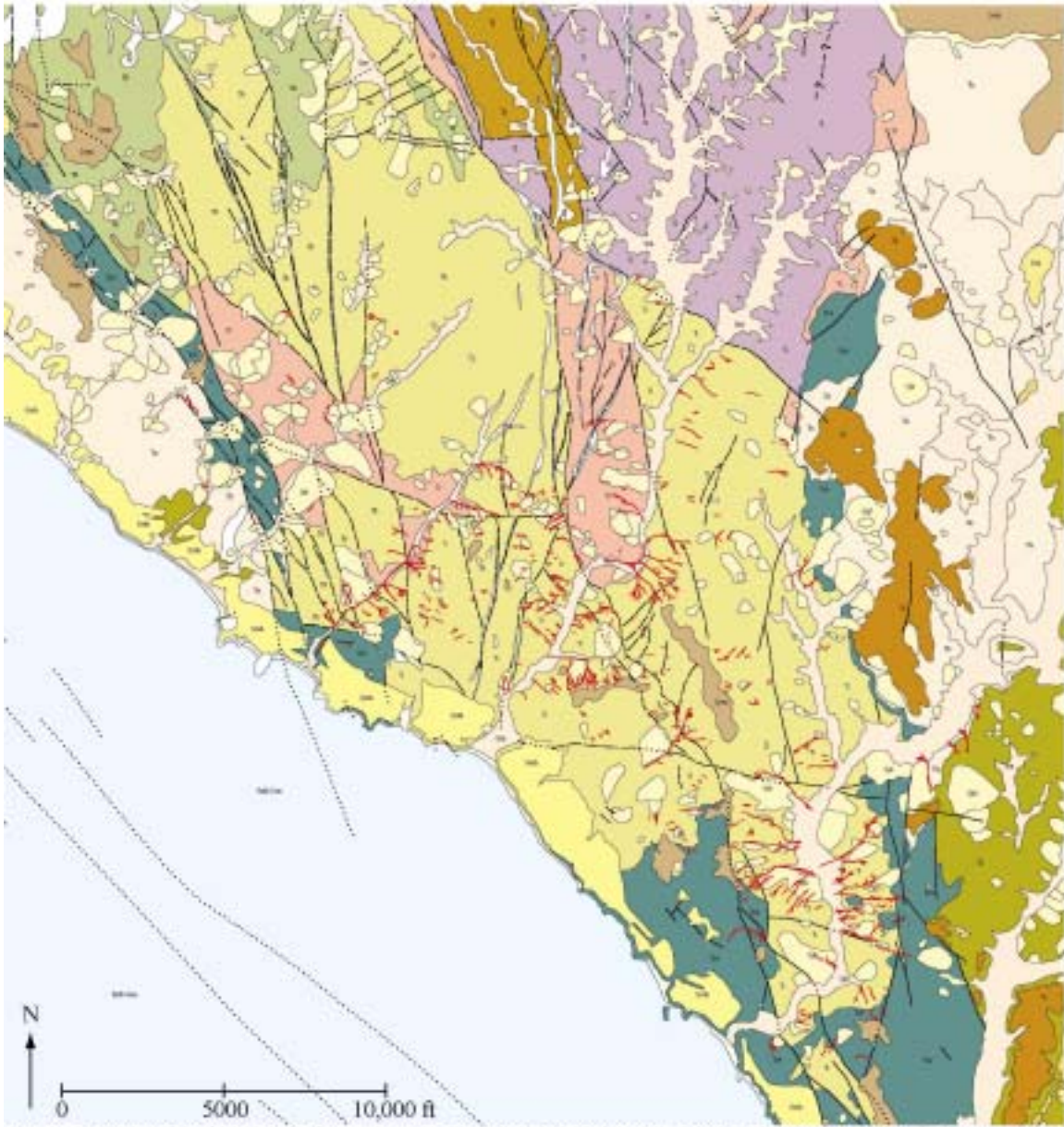


Figure 12 Map showing debris flows, Laguna Beach, Orange County, 1998. Red lines are debris flows. Most debris flows occur within the Topanga Formation (gold color). The longer debris flows traveled 1000 feet. For unit explanation, see Figure 23.



Figure 13 Disintegrated debris flow, Las Cruces area, Santa Barbara County, 1998.



Figure 14 Debris flow deposit in channel, Laguna Beach area, Orange County, 1998.



Figure 15 Debris flow deposited on small alluvial fan, Santa Monica Mountains, Los Angeles County, 1980. Brown roofed house near center built on a small alluvial fan was damaged by a relatively small debris flow.



Figure 16 Debris flow deposited on small alluvial fan, Santa Monica Mountains, Los Angeles County, 1980, damaged the two houses built on the apex of the fan.



Figure 17 Structural damage produced by debris flows, Laguna Canyon, Orange County, 1998.



Figure 18 Structural damage produced by debris flows, Laguna Canyon, Orange County, 1998.

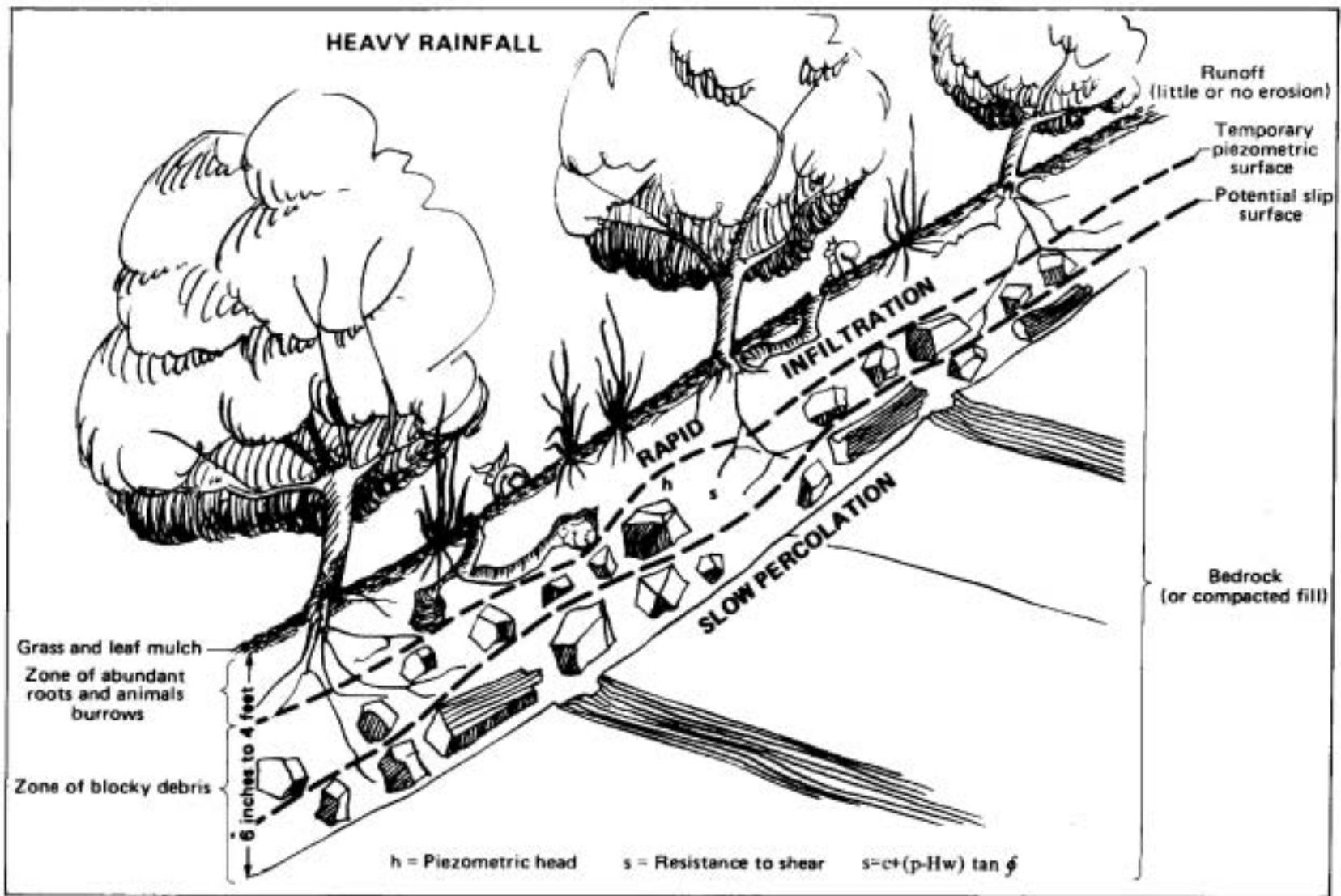


Figure 19 Sketch showing buildup of perched water table in colluvial soil during heavy rainfall. From Campbell, 1975.



Figure 20 Relatively large disintegrated debris flow deposited on hillside, Las Cruces area, Santa Barbara County, 2001. Note road for scale.

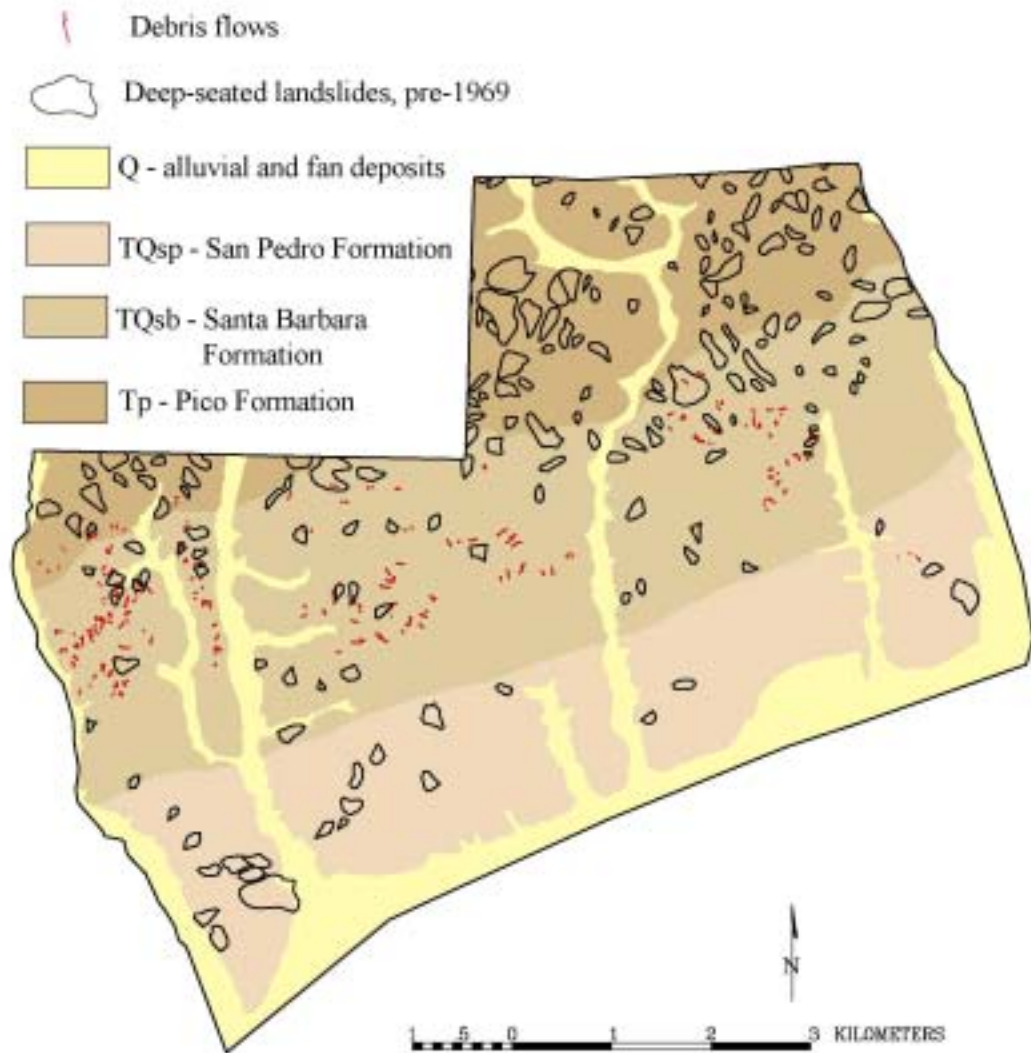


Figure 21 Distribution of debris flows produced during 2001 winter rains, Santa Paula area, Ventura County. Rainfall threshold was exceeded for the Santa Barbara Formation and being reached for the San Pedro and Pico Formations. Note only a few debris flows occurred in pre-existing landslides.

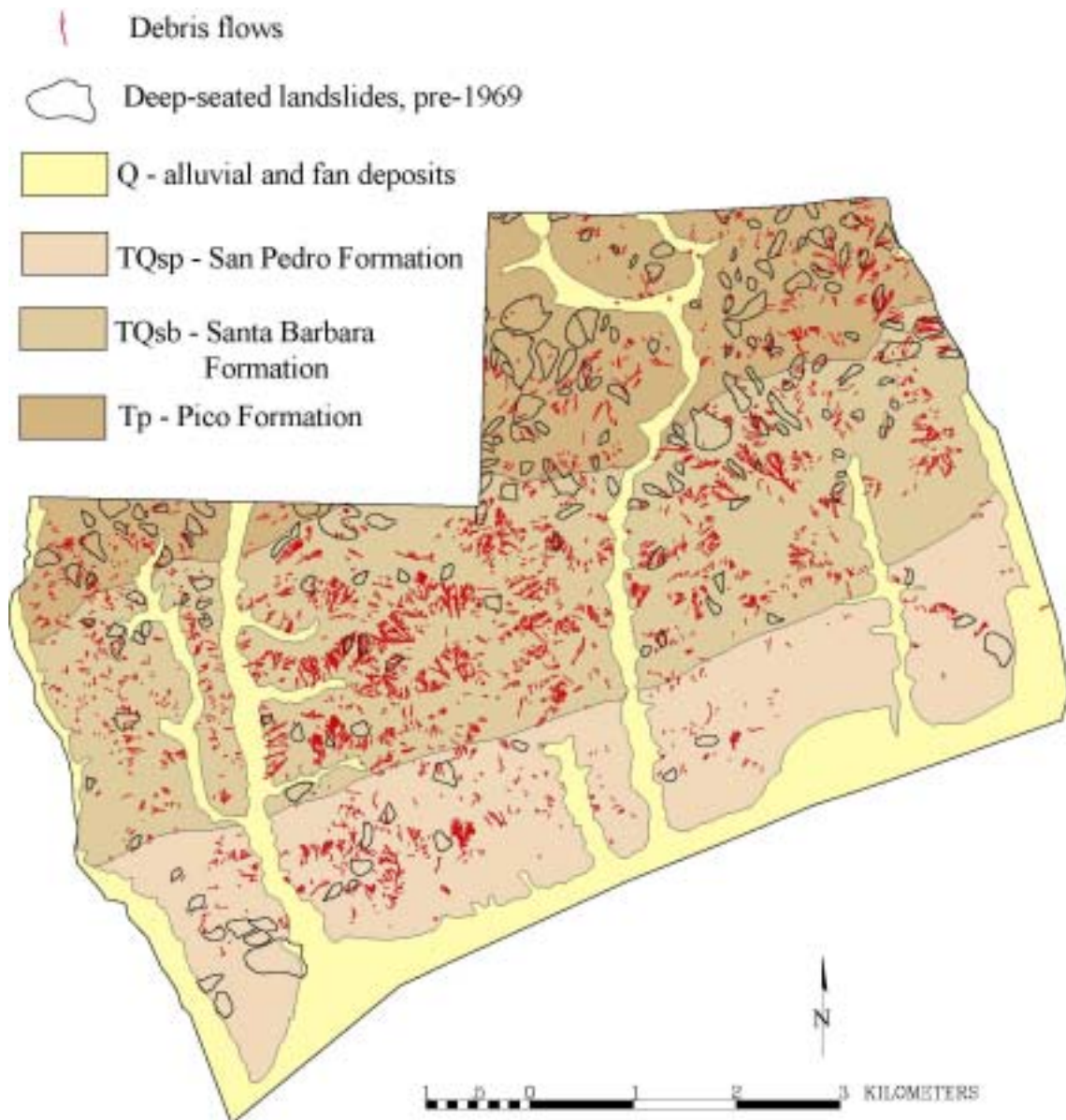


Figure 22 Distribution of debris flows produced during 1998 'El Niño' winter rains, Santa Paula area, Ventura County. In contrast to 2001 (Figure 21) rainfall threshold was exceeded for the Santa Barbara Formation, San Pedro and Pico Formations. From Hauser, 2000.

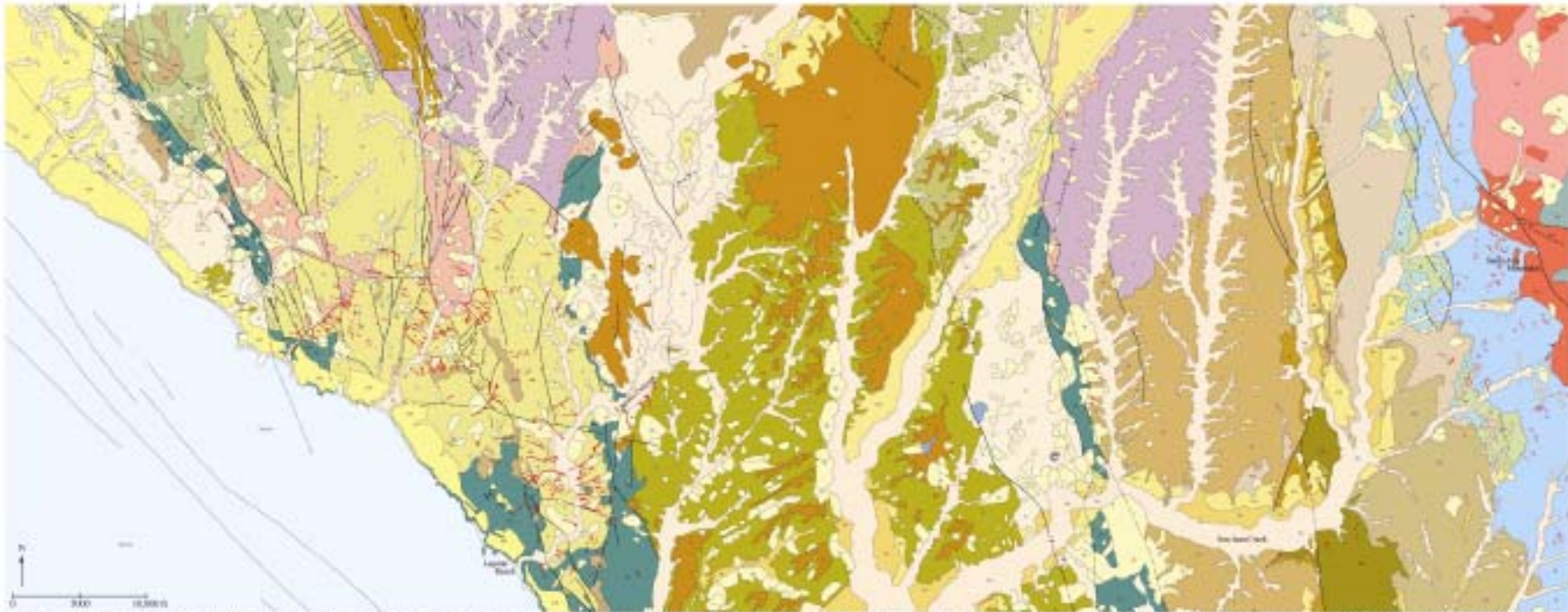


Figure 25. Geologic map of the Laguna Death-Barro Alto Mountains area, Georgia County showing debris flows, soil lines, that was produced during 1998. Geology from Morton, 1997. Threshold contour was closely excluded for triggering soil slip debris flows in the Tappan Formation (undifferentiated Tappan Formation - T1 and the Gwynne Member - T6), but not the Lee Vance Member - Tiffind and Wilcox Formation - T9. The debris flows originating in the Tappan Formation are of relatively long length, up to one mile in length, compared to the relatively short length of those of the Wilcox Formation. The threshold was being searched for the San Ochoa Basins - T6b, the Pleasant Sandstone Member - Kays, Schick Ranch Sandstone Member - Kays, and Star Member - lower of the Williams Formation, and the Baker Canyon Member - K2b of the Ladd Formation. Baker Canyon Member - K2b. Note the Wilcox Formation (the presence numerous bedrock landslides produced by debris flows).  
 Geologic map units - This debris flow inventory dataset compiled 28 geologic map units. Q6 - Holocene landslides deposits, Q5a - Young soil channel deposits, Q5a - Old soil channel deposits, Q5a - Very old soil channel deposits, Q5a - Old marine deposits, Q5a - Very old marine deposits, Q5a - Very old alluvial fan deposits, T1 - Tappan Formation, Gwynne Member, T2 - Tappan Formation, Gwynne Member, T3 - Tappan Formation, Gwynne Member, T4 - Tappan Formation, Gwynne Member, T5 - Tappan Formation, Gwynne Member, T6 - Tappan Formation, Gwynne Member, T7 - Tappan Formation, Gwynne Member, T8 - Tappan Formation, Gwynne Member, T9 - Tappan Formation, Gwynne Member, T10 - Tappan Formation, Gwynne Member, T11 - Tappan Formation, Gwynne Member, T12 - Tappan Formation, Gwynne Member, T13 - Tappan Formation, Gwynne Member, T14 - Tappan Formation, Gwynne Member, T15 - Tappan Formation, Gwynne Member, T16 - Tappan Formation, Gwynne Member, T17 - Tappan Formation, Gwynne Member, T18 - Tappan Formation, Gwynne Member, T19 - Tappan Formation, Gwynne Member, T20 - Tappan Formation, Gwynne Member, T21 - Tappan Formation, Gwynne Member, T22 - Tappan Formation, Gwynne Member, T23 - Tappan Formation, Gwynne Member, T24 - Tappan Formation, Gwynne Member, T25 - Tappan Formation, Gwynne Member, T26 - Tappan Formation, Gwynne Member, T27 - Tappan Formation, Gwynne Member, T28 - Tappan Formation, Gwynne Member, T29 - Tappan Formation, Gwynne Member, T30 - Tappan Formation, Gwynne Member, T31 - Tappan Formation, Gwynne Member, T32 - Tappan Formation, Gwynne Member, T33 - Tappan Formation, Gwynne Member, T34 - Tappan Formation, Gwynne Member, T35 - Tappan Formation, Gwynne Member, T36 - Tappan Formation, Gwynne Member, T37 - Tappan Formation, Gwynne Member, T38 - Tappan Formation, Gwynne Member, T39 - Tappan Formation, Gwynne Member, T40 - Tappan Formation, Gwynne Member, T41 - Tappan Formation, Gwynne Member, T42 - Tappan Formation, Gwynne Member, T43 - Tappan Formation, Gwynne Member, T44 - Tappan Formation, Gwynne Member, T45 - Tappan Formation, Gwynne Member, T46 - Tappan Formation, Gwynne Member, T47 - Tappan Formation, Gwynne Member, T48 - Tappan Formation, Gwynne Member, T49 - Tappan Formation, Gwynne Member, T50 - Tappan Formation, Gwynne Member, T51 - Tappan Formation, Gwynne Member, T52 - Tappan Formation, Gwynne Member, T53 - Tappan Formation, Gwynne Member, T54 - Tappan Formation, Gwynne Member, T55 - Tappan Formation, Gwynne Member, T56 - Tappan Formation, Gwynne Member, T57 - Tappan Formation, Gwynne Member, T58 - Tappan Formation, Gwynne Member, T59 - Tappan Formation, Gwynne Member, T60 - Tappan Formation, Gwynne Member, T61 - Tappan Formation, Gwynne Member, T62 - Tappan Formation, Gwynne Member, T63 - Tappan Formation, Gwynne Member, T64 - Tappan Formation, Gwynne Member, T65 - Tappan Formation, Gwynne Member, T66 - Tappan Formation, Gwynne Member, T67 - Tappan Formation, Gwynne Member, T68 - Tappan Formation, Gwynne Member, T69 - Tappan Formation, Gwynne Member, T70 - Tappan Formation, Gwynne Member, T71 - Tappan Formation, Gwynne Member, T72 - Tappan Formation, Gwynne Member, T73 - Tappan Formation, Gwynne Member, T74 - Tappan Formation, Gwynne Member, T75 - Tappan Formation, Gwynne Member, T76 - Tappan Formation, Gwynne Member, T77 - Tappan Formation, Gwynne Member, T78 - Tappan Formation, Gwynne Member, T79 - Tappan Formation, Gwynne Member, T80 - Tappan Formation, Gwynne Member, T81 - Tappan Formation, Gwynne Member, T82 - Tappan Formation, Gwynne Member, T83 - Tappan Formation, Gwynne Member, T84 - Tappan Formation, Gwynne Member, T85 - Tappan Formation, Gwynne Member, T86 - Tappan Formation, Gwynne Member, T87 - Tappan Formation, Gwynne Member, T88 - Tappan Formation, Gwynne Member, T89 - Tappan Formation, Gwynne Member, T90 - Tappan Formation, Gwynne Member, T91 - Tappan Formation, Gwynne Member, T92 - Tappan Formation, Gwynne Member, T93 - Tappan Formation, Gwynne Member, T94 - Tappan Formation, Gwynne Member, T95 - Tappan Formation, Gwynne Member, T96 - Tappan Formation, Gwynne Member, T97 - Tappan Formation, Gwynne Member, T98 - Tappan Formation, Gwynne Member, T99 - Tappan Formation, Gwynne Member, T100 - Tappan Formation, Gwynne Member.

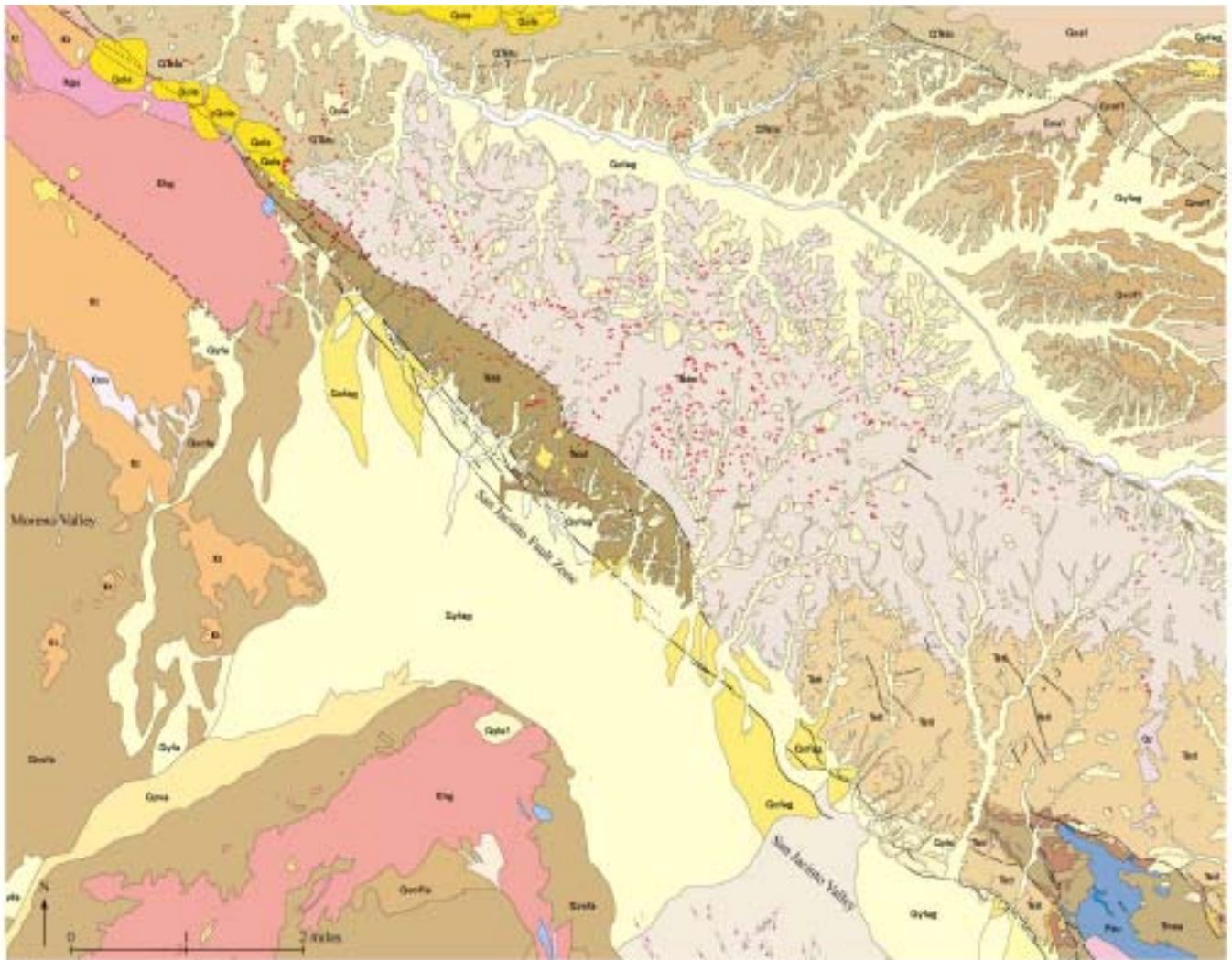


Figure 24 Distribution of debris flows, shown in red, San Timoteo Butte, Riverside County. Rainfall threshold was clearly exceeded for the upper (Qf1a) and middle members (T1m, T1d) of the San Timoteo Beds, and was being attained for the lower member (T1l) and landslides (Qh). Threshold was not reached for other geologic units (granite rocks (Kt, Kbg), metamorphic rocks (Psa, m), older sedimentary units (T1ca) and older alluvial fan deposits (Qvff).

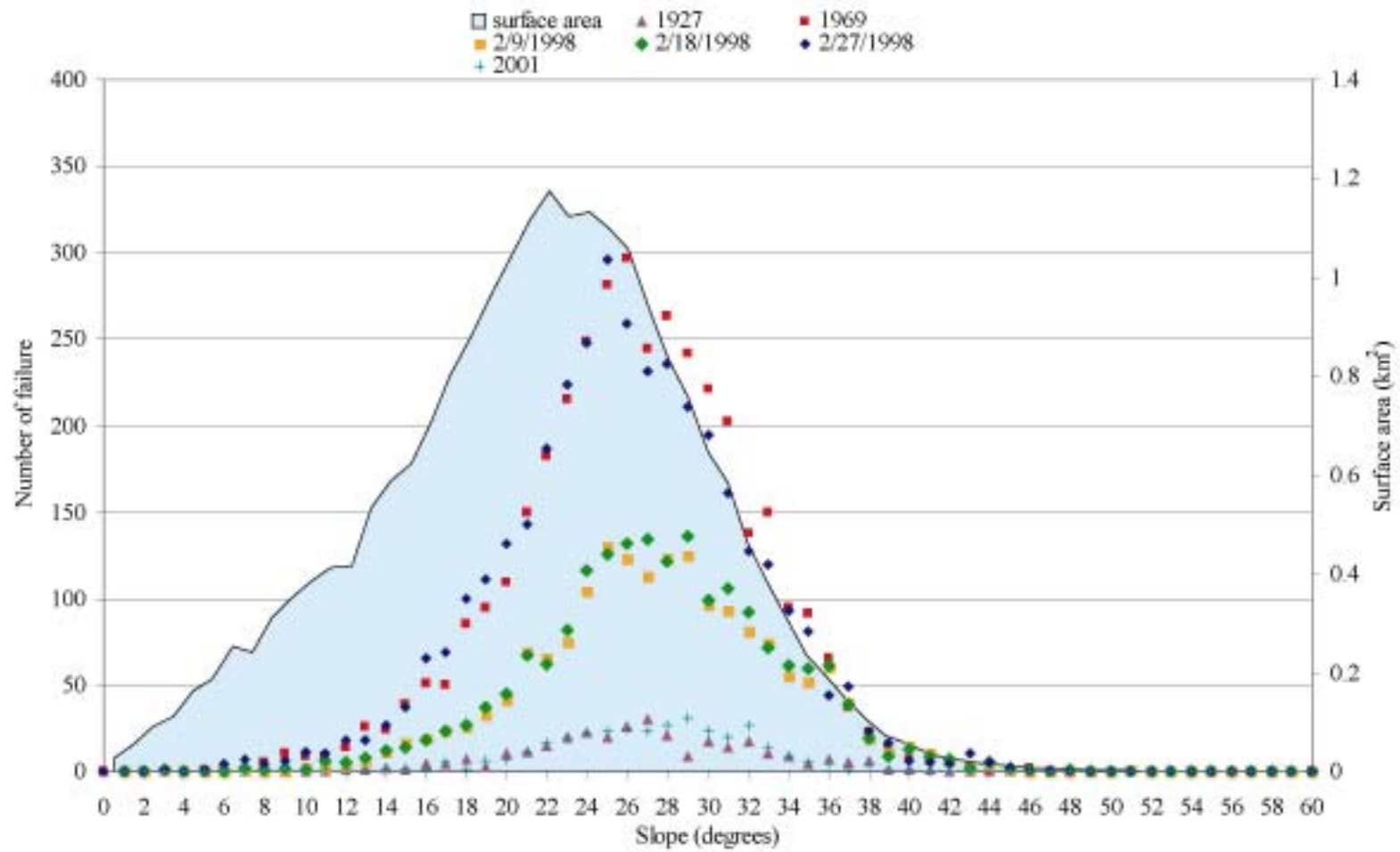


Figure 25 Plot of slope frequency and soil slip frequency in the Santa Paula area, Ventura County for debris flows generated during the winters of 1927, 1969, 1998, and 2001. Modified from Hauser, 2000.

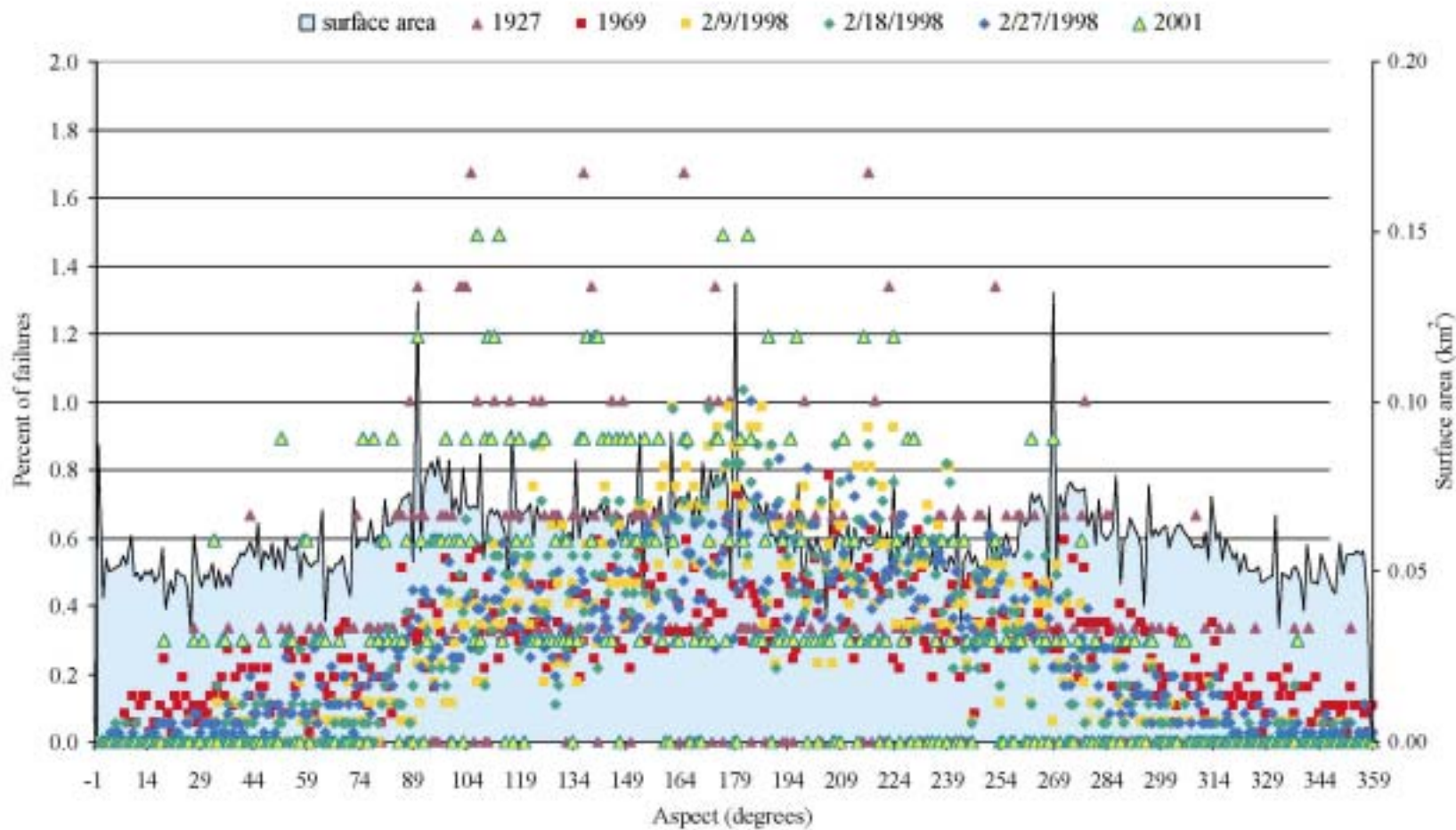


Figure 26 Plot of aspect frequency and soil slip frequency in the Santa Paula area, Ventura County for debris flows generated during the winters of 1927, 1969, 1998, and 2001. Modified from Hauser, 2000.



Figure 27 San Timoteo Badlands, Riverside County, 1983. View is to the west. More debris flows occurred on south facing slopes than on north facing slopes. Note how high on the ridges the debris flows start.



Figure 28 Santa Monica Mountains, Los Angeles County, 1980. View is to the west. More debris flows occurred on south facing slopes than on north facing slopes. Note the difference in vegetation between the north-and south-facing slopes.

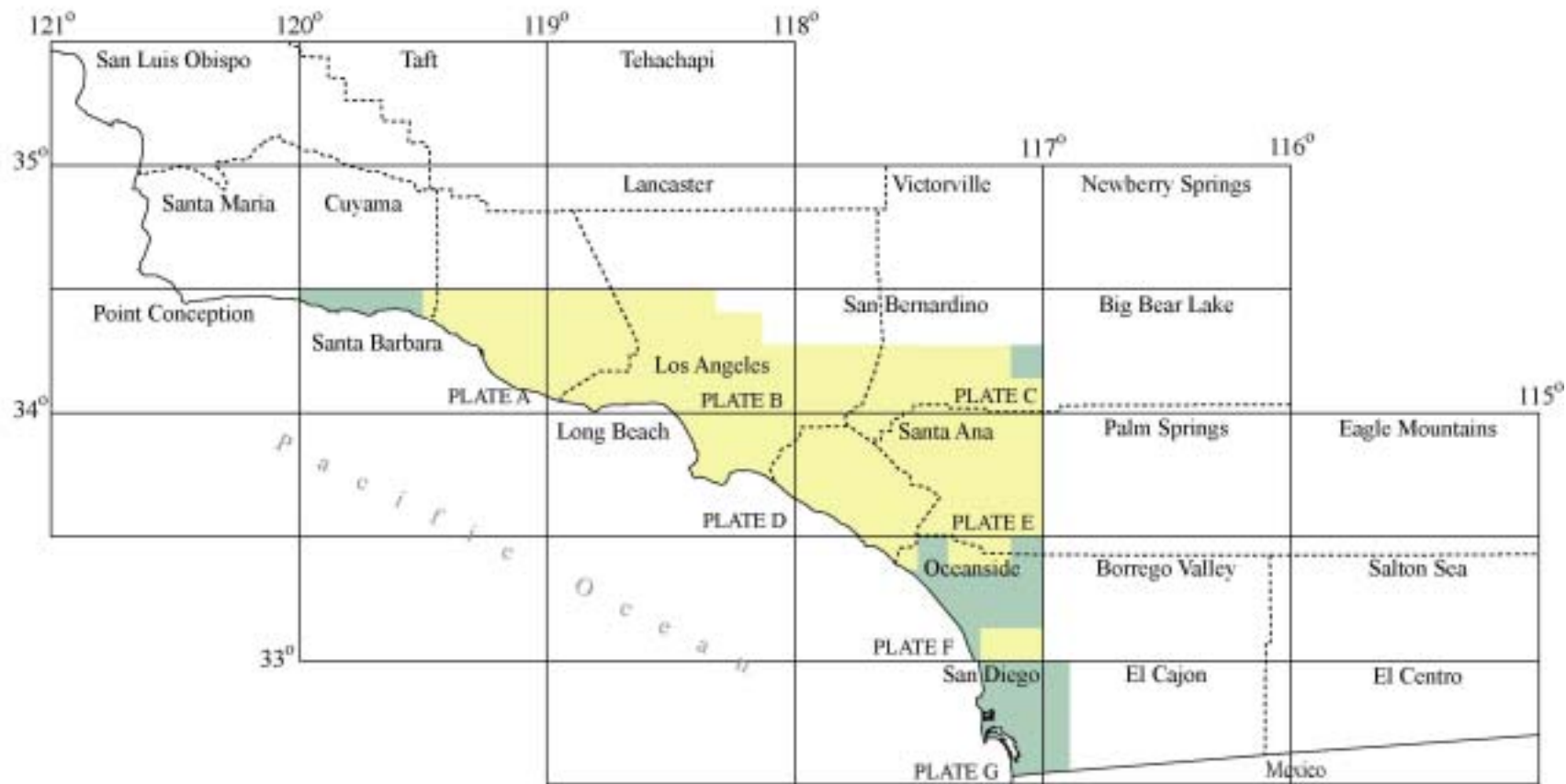


Figure 29 Index map of the Southern California Areal Mapping Project area (SCAMP) showing location of 10-meter (yellow shaded areas) and 30-meter (green shaded areas) DEMs used in the soil-slip susceptibility analysis.

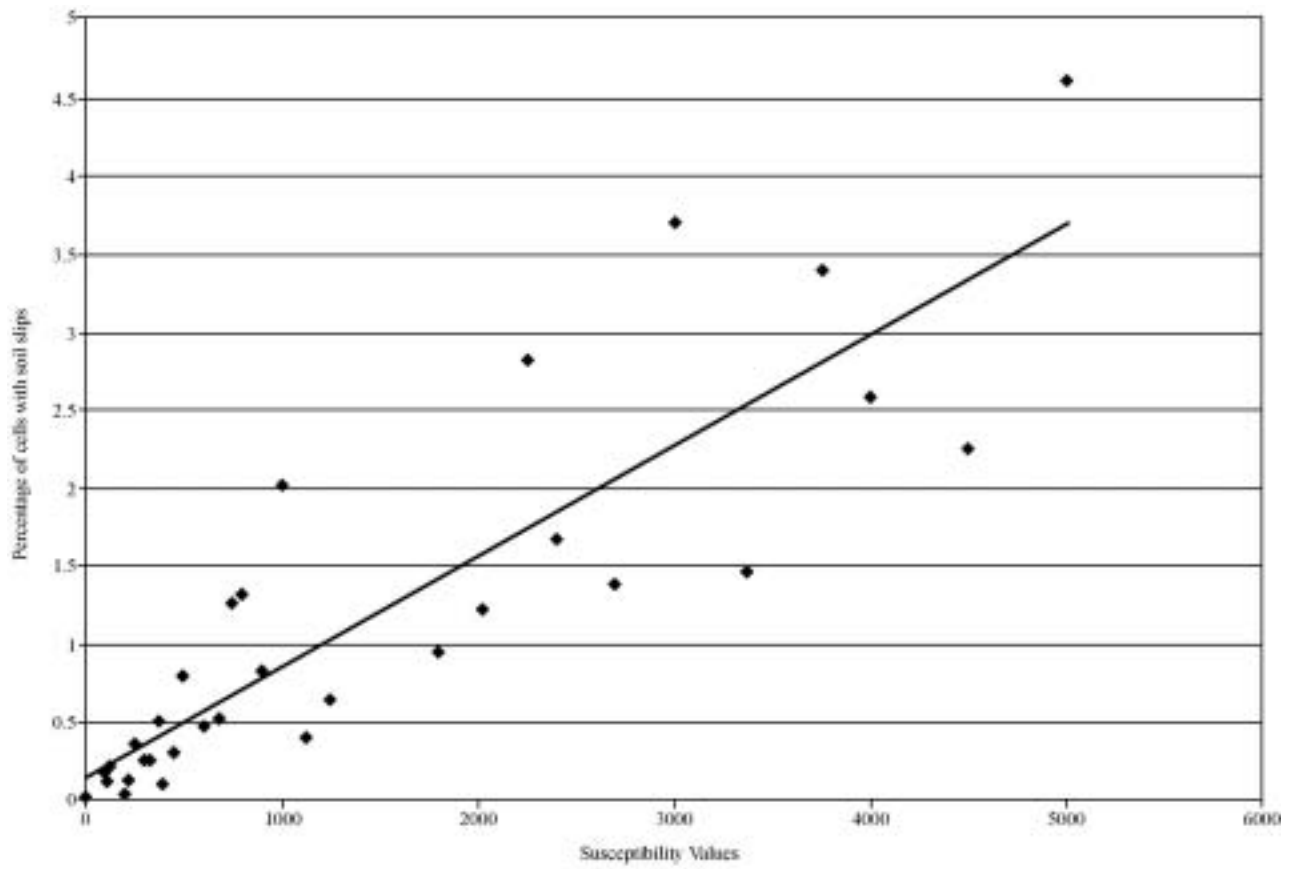


Figure 30 Plot of the percentage of cells with soil slips by susceptibility value, Santa Paula area, 1998 soil slips.

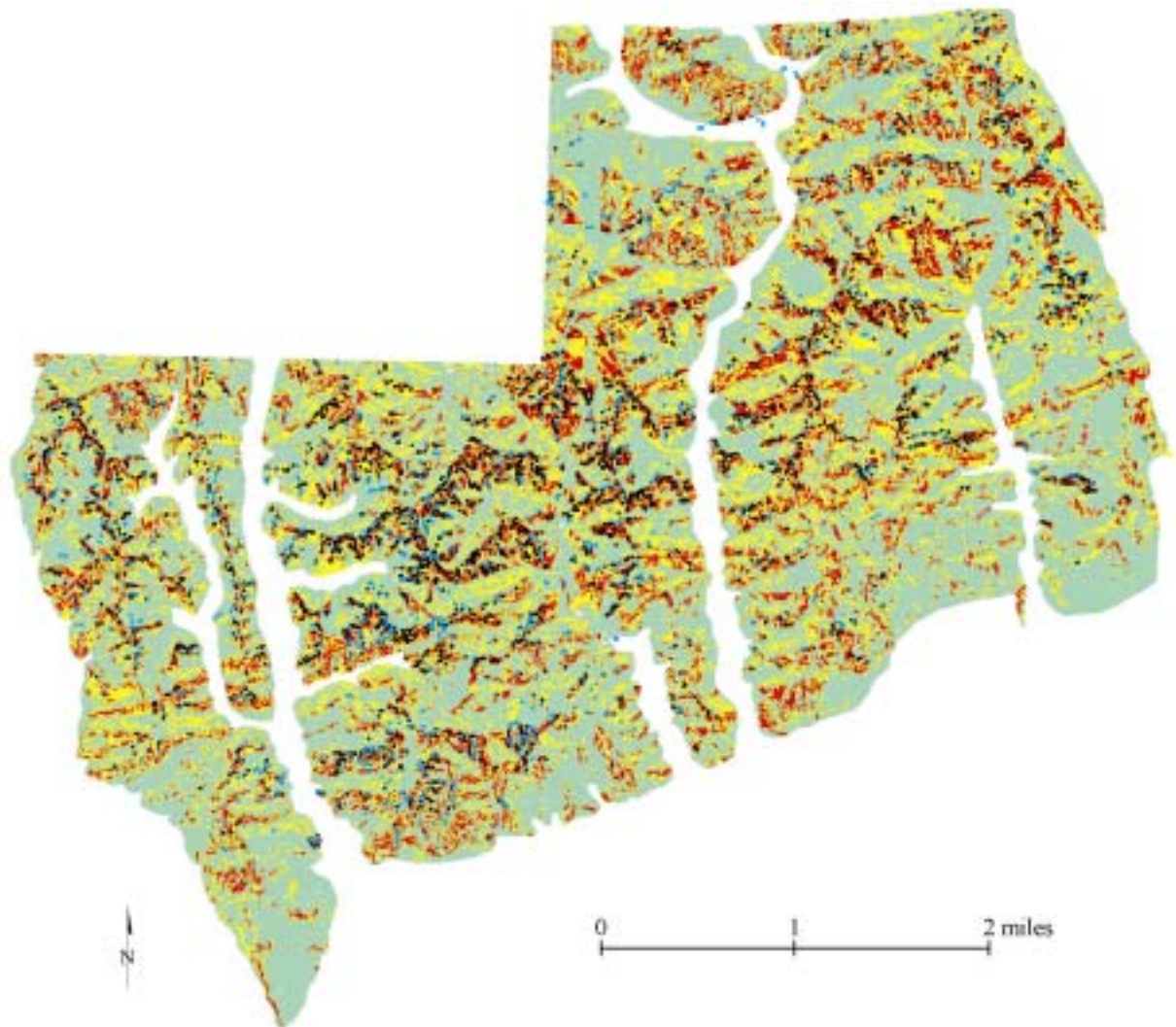


Figure 31 Map showing soil-slip susceptibility units and soil-slip sites, Santa Paula area, Ventura County. Green designates low soil-slip susceptibility, yellow moderate susceptibility and red high susceptibility. Soil slips originating in moderate and high susceptibility cells are black dots; those originating in low susceptibility cells are blue dots. Note the clustering of blue dots adjacent to high susceptibility cells. The few soil slips in the uncolored upper right corner occurred in steep banks of incised drainages.

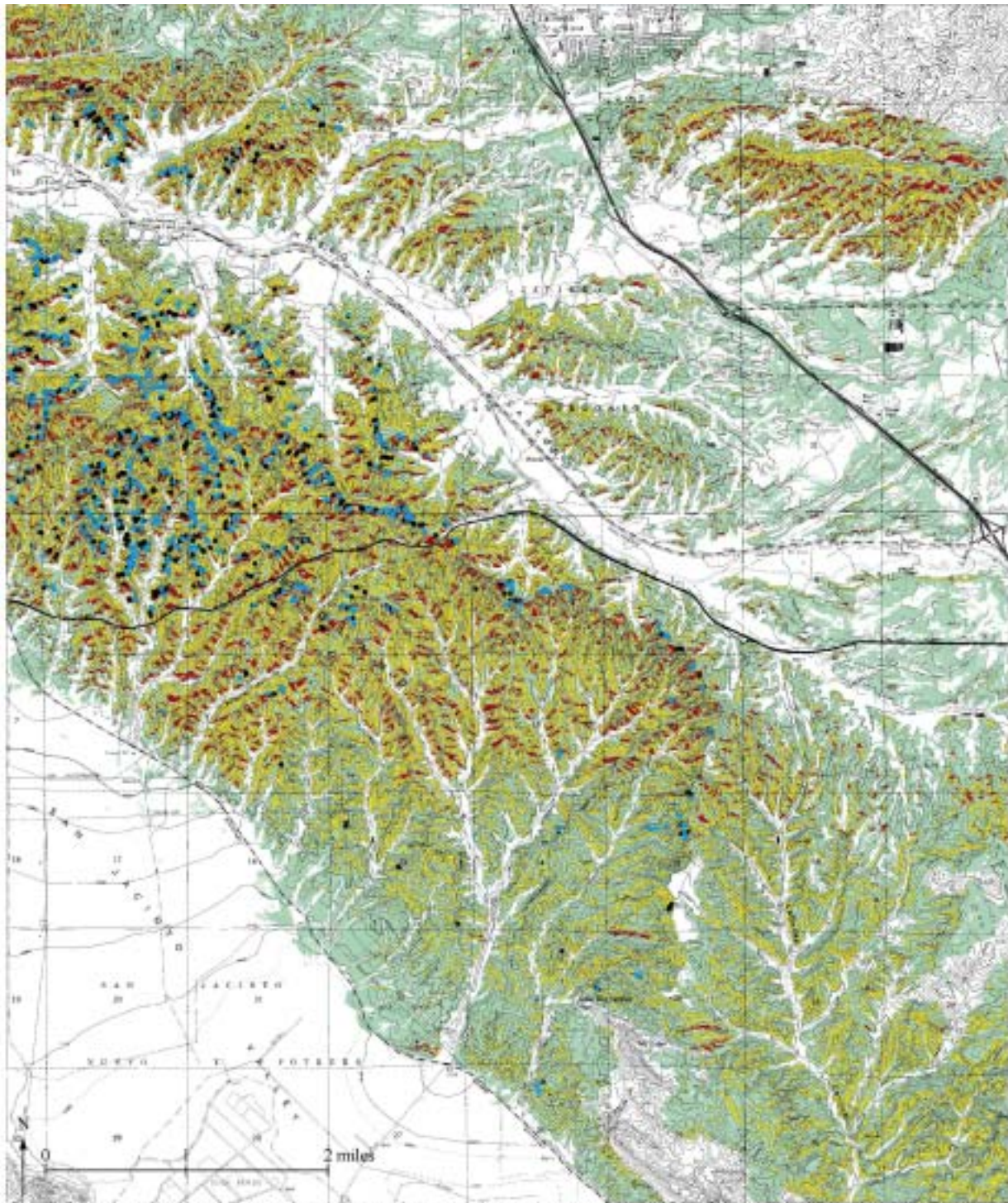


Figure 32 Map showing soil-slip susceptibility units and the location of soil slips, El Casco 7.5' quadrangle, San Timoteo Badlands, Riverside County, 1998. Green designates low soil-slip susceptibility, yellow moderate susceptibility and red high susceptibility. Black dots are soil-slips that occurred within high susceptibility value DEM cells; the blue dots are soil-slips that occurred in low value susceptibility cells mainly immediately up slope from the high value susceptibility cells. Debris flow inventory aerial photography did not include the northeastern part of the quadrangle (i.e., east of Interstate 10). Note the preponderance of soil slips located on south facing slopes.